Eur Biophys J (2007) 36:393–404
DOI 10.1007/s00249-006-0094-2

ARTICLE

Solid-state NMR characterization of the putative membrane anchor of TWD1 from *Arabidopsis thaliana*

Holger A. Scheidt · Alexander Vogel · Andreas Eckhoff · Bernd W. Koenig · Daniel Huster

Received: 5 May 2006 / Revised: 16 August 2006 / Accepted: 25 August 2006 / Published online: 11 October 2006
© EBSA 2006

Abstract Structure and membrane interaction of a 31 amino acid residue fragment of the membrane bound FKBP-like protein twisted dwarf 1 (TWD1) from *Arabidopsis thaliana* was investigated by solid-state NMR spectroscopy. The studied peptide TWD1(335–365) contained the putative membrane anchor of the protein (residues 339–357) that was previously predicted by sequence hydrophobicity analysis. The TWD1 peptide was synthesized by standard solid phase peptide synthesis and contained three uniformly ^{13}C- and ^{15}N-labelled residues (Phe 340, Val 350, Ala 364). The peptide was incorporated into either multilamellar vesicles or oriented planar membranes composed of an equimolar ternary phospholipid mixture (POPC, POPE, POPG), where the POPC was *sn*-1 chain-deuterated. ^{31}P NMR spectra of the membrane in the absence and in the presence of the peptide showed axially symmetric powder patterns indicative of a lamellar bilayer phase. Further, the addition of peptide caused a decrease in the lipid hydrocarbon chain order as indicated by reduced quadrupolar splittings in the ^{2}H NMR spectra of the POPC in the membrane. The conformation of TWD1(335–365) was investigated by ^{13}C cross-polarization magic-angle spinning NMR spectroscopy. At a temperature of −30°C all peptide signals were resolved and could be fully assigned in two-dimensional proton-driven ^{13}C spin diffusion and ^{13}C single quantum/double quantum correlation experiments. The isotropic chemical shift values for Phe 340 and Val 350 exhibited the signature of a regular α-helix. Chemical shifts typical for a random coil conformation were observed for Ala 364 located close to the C-terminus of the peptide. Static ^{15}N NMR spectra of TWD1(335–365) in mechanically aligned lipid bilayers demonstrated that the helical segment of TWD1(335–365) adopts an orientation perpendicular to the membrane normal. At 30°C, the peptide undergoes intermediate time scale motions.

Introduction

A number of important biological functions take place at cellular membranes. These processes are mediated by protein–protein interactions and biochemical reactions. Membrane association of the interaction partners dramatically increases the likelihood of intermolecular contacts (Marshall 1993). When membrane-associated, the protein diffusion is restricted to two dimensions, which increases the effective protein concentration by about a factor of 1,000 compared to free diffusion in the cytosol (Murray et al. 1997). Nature has devised several ways for membrane anchoring of proteins. Common structural motives include transmembrane (TM) α-helices (White and von Heijne 2005), covalently attached lipid alkyl

Dedicated to Prof. K. Arnold on the occasion of his 65th birthday.

H. A. Scheidt · A. Vogel · D. Huster (✉)
Junior Research Group "Structural Biology of Membrane Proteins", Institute of Biotechnology,
Martin Luther University Halle-Wittenberg,
Kurt-Mothes-Str. 3, 06120 Halle, Germany
e-mail: daniel.huster@biochemtech.uni-halle.de

A. Eckhoff · B. W. Koenig
Structural Biology Institute, IBI-2, Research Centre Jülich,
52425 Jülich, Germany

B. W. Koenig
Physical Biology Institute, Heinrich Heine University
Düsseldorf, 40225 Dusseldorf, Germany

chains (Casey 1995), and GPI-anchors (Ikezawa 2002). Membrane anchors may be identified in the protein primary structure by hydrophobicity analysis (White and Wimley 1999) or by screening for specific recognition sequences (Hancock et al. 1991).

TWD1 is a multidomain FKBP-like membrane protein from *Arabidopsis thaliana*. Mutants of *Arabidopsis* that lack the TWD1 gene show a drastic pleiotropic phenotype with reduced cell elongation, diminished overall size, and disoriented growth of all organs (Geisler et al. 2003; Geisler et al. 2004; Kamphausen et al. 2002). Gene analysis of TWD1 revealed one FKBP domain, one TPR domain with three motives, a putative calmodulin binding domain, and a hydrophobic C-terminal region (residues 339–357) that very likely serves as membrane anchor (Kamphausen et al. 2002). The predicted topology of TWD1 is given in Fig. 1. Currently there are 29 annotated *Arabidopsis* genes that code for FKBP-type PPIases. Among those only the TWD1 gene contains a sequence that codes for a putative membrane anchor, consisting of a highly hydrophobic stretch of 19 residues close to the C-terminus (residues 339–357). In general there are only very few FKBPs, for which a membrane anchor was predicted by gene analysis. However, only in the case of TWD1 the membrane location of the protein was confirmed experimentally. First, immunogold-labelling of TWD1 followed by electron microscopy as well as membrane separation techniques combined with Western blotting analysis revealed a dual location of TWD1, which was found to reside in plasma and vacuolar membranes (Geisler et al. 2003; Kamphausen et al. 2002). Second, release of full length TWD1 from microsomal membranes required harsh treatment with membrane solubilizing concentrations of detergent indicating a transmembrane rather than a peripheral location (Geisler et al. 2003).

There is evidence for intimate molecular interaction of the FKBP domain of TWD1 with multidrug resistance-like ABC transporters *At*PGP1 and *At*PGP19, which are located in the plasma membrane (Geisler et al. 2003). A regulatory role of TWD1 on *At*PGP1/*At*PGP19 transport activities and perhaps on polar auxin transport has been suggested (Geisler et al. 2003). Very recently, an interaction between the TPR domain of TWD1 and the vacuolar ABC transporters *At*MRP1 and *At*MRP2 was demonstrated and a role of TWD1 as modulator of vacuolar substrate uptake was proposed (Geisler et al. 2004).

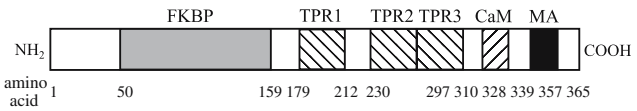

Fig. 1 Schematic domain structure of the TWD1-protein: *FKBP* FKBP-like domain, *TPR* tetratricopeptide repeat, *CaM* putative calmodulin binding region, *MA* membrane anchor

The C-terminal membrane anchor of TWD1 may simply increase the probability of contacts between TWD1 and its membrane-based molecular targets by reducing the dimensionality of TWD1 diffusion. Further, TWD1 serves as a regulator of several different transporters with individual substrate specificity that are located on separate membranes. Restraining the mobility of TWD1 to a membrane might serve as a means to decouple regulation of transporters located on different membranes.

A high-resolution structure of TWD1 would certainly advance the understanding of the molecular interactions of TWD1 with its known partners. Successful crystallization and preliminary X-ray crystallographic analysis of the N-terminal fragment TWD1(1–180) has been reported (Eckhoff et al. 2005 1,773/id). Very recently, the three-dimensional structure of the N-terminal FKBP-like domain of TWD1 was solved (Weiergraber et al. 2006). However, attempts to crystallize the full-length multidomain protein TWD1 including the membrane anchor have not been successful so far.

The determination of atomically resolved structures of membrane proteins still remains a big challenge in structural biology (Torres et al. 2003). Nevertheless, solid-state NMR techniques have advanced considerably over the last few years and allow now determination of structural models of membrane proteins even in liquid-crystalline membranes (Davis and Auger 1999; Huster 2005; Luca et al. 2003; Opella and Marassi 2004; Thompson 2002). Solid-state NMR spectroscopy has been particularly successful in the determination of structures of small membrane proteins and of segments from larger membrane proteins (Afonin et al. 2004; Andronesi et al. 2005; Huster et al. 2003; Ketchem et al. 1993; Reuther et al. 2006; Sharpe et al. 2006; Smith et al. 2001; Wagner et al. 2004; Yang and Weliky 2003; Zhang et al. 2003). In addition solid-state NMR investigations contributed significantly to the understanding of the membrane interaction of different antimicrobial peptides (Bechinger 1999; Henzler-Wildman et al. 2003; Porcelli et al. 2006).

Here, we investigate the structure and topology of the putative membrane anchor of TWD1 to gain some insight into the mechanism of membrane binding of the whole protein. In addition to confirming the membrane affinity of residues 339–357, we investigated the structure and topology of the membrane anchor of TWD1. Solid-state NMR results are reported that provide insight into the interaction of a C-terminal fragment of

TWD1 comprising amino acid residues 335–365 with a phospholipid membrane. The data strongly support an α-helical structure of the central and very hydrophobic region of the peptide. TWD1(335–365) appears to be located in the lipid water interface region of the membrane and aligns with the long axis of the helix parallel to the membrane surface.

Materials and methods

Materials

The lipids 1-palmitoyl-2-oleoyl-*sn*-glycero-3-phosphocholine (POPC), 1-palmitoyl-d_{31}-2-oleoyl-*sn*-glycero-3-phosphocholine (POPC-d_{31}), 1-palmitoyl-2-oleoyl-*sn*-glycero-3-[phospho-*rac*-(1-glycerol)] (sodium salt) (POPG) and 1-palmitoyl-2-oleoyl-*sn*-glycero-3-phosphoethanolamine (POPE) were purchased from Avanti Polar Lipids, Inc. (Alabaster, AL, USA) and used without further purification. Uniformly ^{13}C- and ^{15}N-labelled amino acids were purchased from Cambridge Isotope Laboratories, Inc. (Andover, MA, USA). The peptide TWD1(335–365) with the amino acid sequence KSKSL **F**WLIVLWQWF **V**SLFSRIFRR HRVK**A**D, a protonated N- and an amidated C-terminus was synthesized at the medical Faculty (Charité) of the Humboldt University Berlin using standard Fmoc peptide synthesis. The uniformly ^{13}C/^{15}N-labelled amino acids were introduced at positions Phe 340, Val 350 and Ala 364.

Sample preparation

Appropriate amounts of TWD1(335–365) and phospholipids (molar ratio POPC-d_{31}/POPE/POPG 1:1:1) were co-dissolved in a chloroform–methanol mixture. The molar peptide-to-lipid ratio was 1:30. After solvent evaporation the sample prepared for NMR measurements on multilamellar vesicles was re-dissolved in cyclohexane and lyophilized at high vacuum to obtain a fluffy powder. After hydration with 35 wt% buffer solution (10 mM HEPES, 10 mM NaCl, pH 7.4) the sample was equilibrated by freeze–thaw cycles and gentle centrifugation. The sample was transferred into a 4 mm MAS rotor with Teflon inserts (50 µl volume) for NMR measurements.

For the ^{15}N NMR measurements the chloroform–methanol solution of TWD1(335–365) and phospholipids was spread onto glass plates (7 mm × 10 mm, 0.04 mg/mm^2) and slowly dried overnight at 500 mbar (Seul and Sammon 1990). The samples were hydrated for at least 24 h via the vapor phase of a saturated $CaSO_4$ solution providing a relative humidity of 98%. The glass plates were stacked, wrapped in parafilm, and sealed in an air-tight plastic bag. The crystalline reference sample was prepared from approximately 15 mg of dry TWD1(335–365).

Static ^{2}H and ^{31}P NMR spectroscopy

Static ^{31}P NMR spectra of membrane phospholipids were acquired at 30°C on a Bruker DRX 600 NMR spectrometer (Bruker Biospin, Rheinstetten, Germany) operating at a ^{31}P resonance frequency of 242.9 MHz using a spin echo pulse sequence (Hahn 1950). A ^{31}P 90° pulse length of 7 µs, a spin echo delay time of 50 µs, a spectral width of 100 kHz, and a recycle delay of 2 s were used. Continuous-wave proton decoupling was applied during signal acquisition. The experimental spectra were simulated using a program written in Mathcad 2001 (MathSoft, Inc., Cambridge, MA, USA) to obtain the chemical shift anisotropy (CSA).

Static ^{2}H NMR spectra were recorded at 30°C on a Bruker Avance 400 NMR spectrometer operating at a ^{2}H resonance frequency of 61.2 MHz. A dual resonance solids probe with a 5 mm solenoid coil was used. The ^{2}H NMR spectra were acquired at a spectral width of 500 kHz using a phase-cycled quadrupolar echo sequence (Davis et al. 1976) comprised of two 3 µs 90° pulses that were separated by a 60 µs delay. The relaxation delay between scans was 500 ms. The ^{2}H NMR spectra were dePaked and analysed as described in detail in (Huster et al. 1998). Smoothed chain order parameter profiles were calculated using the standard procedure (Lafleur et al. 1989).

^{13}C MAS NMR experiments

All ^{13}C MAS NMR experiments were carried out on a Bruker Avance 750 NMR spectrometer operating at a resonance frequency of 749.7 MHz for ^{1}H and 188.5 MHz for ^{13}C. A double-resonance MAS probe equipped with a 4 mm spinning module was used. The ^{13}C 90° pulse length was typically 5–6 µs. CP MAS spectra were acquired with a ^{1}H 90° pulse length of 4 µs and a CP contact time of 700 µs. The ^{1}H radio-frequency field strength during heteronuclear decoupling using TPPM (Bennett et al. 1995) was ~65 kHz. ^{13}C chemical shifts were referenced with respect to external standards: the ^{13}C=O signal of ^{13}C-labelled Gly at 176.45 ppm and the adamantane signals at 38.48 and 29.46 ppm. All ppm values are relative to TMS (Morcombe and Zilm 2003).

Two-dimensional (2D) ^{13}C–^{13}C correlation spectra were obtained using a proton-driven spin diffusion mixing

scheme (Szeverenyi et al. 1982) at a mixing time of 100 ms. The ^{13}C single quantum ^{13}C double quantum correlation spectrum of the INADEQUATE type (Incredible Natural Abundance Double Quantum Transfer) was acquired using the SPC-5 recoupling sequence (Hohwy et al. 1999) for double quantum excitation and reconversion (set to 0.48 ms). The 2D experiments were conducted at temperatures of −30 or 30°C and the MAS frequency was 7,000 or 8,333 Hz.

Static ^{15}N CP NMR experiments on oriented and powder samples

Static ^{15}N CP NMR experiments were performed on the Bruker Avance 750 spectrometer. The ^{15}N resonance frequency on this instrument was 76.0 MHz. A double channel flat coil probe with a coil cross-section of 3 mm × 8 mm and a length of 10 mm was used. The typical 90° ^{15}N pulse length was 10 µs. ^{15}N chemical shifts were referenced based on the N-t-BOC-Gly resonance at 81 ppm. For heteronuclear TPPM decoupling ^{1}H radio-frequency field strength of ∼60 kHz was applied. The glass plates were oriented with the normal parallel to the external magnetic field. The powder-type samples were investigated in a dual channel 4-mm MAS probe at no spinning using similar parameters. All ^{15}N NMR spectra were recorded at a temperature of 30°C.

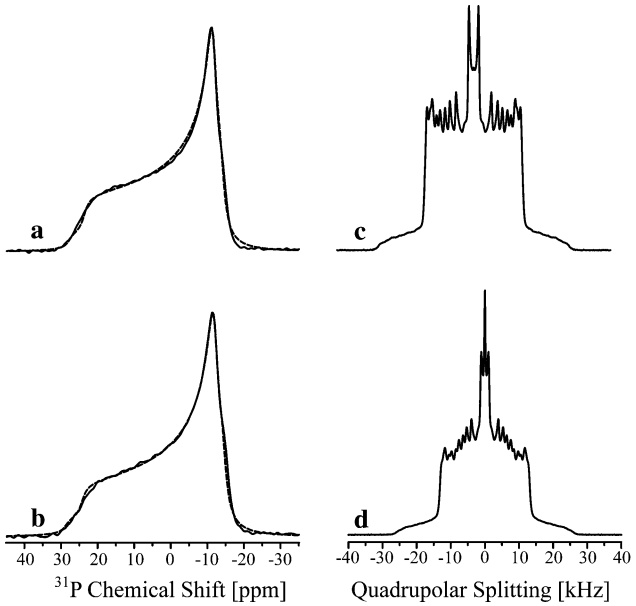

Fig. 2 Influence of TWD1(335–365) incorporation on the lipid membrane. *Left column* Proton-decoupled 242.9 MHz ^{31}P NMR spectra of multilamellar POPC-d_{31}/POPE/POPG vesicles (molar ratio 1:1:1) in the absence (**a**) and in the presence (**b**) of 3.2 mol% TWD1(335–365). Numerical simulations of the spectra are shown as *dashed lines*. *Right column* 61.2 MHz ^{2}H NMR spectra of POPC-d_{31} in equimolar POPC-d_{31}/POPE/POPG vesicles in the absence (**c**) and in the presence (**d**) of 3.2 mol% TWD1(335–365). Measurements were performed in 35 wt% buffer (10 mM NaCl, 10 mM Hepes, pH 7.4) at 30°C

Results

Phase state and lipid packing of TWD1(335–365) containing membranes

The POPC-d_{31}/POPE/POPG (1:1:1 molar ratio) lipid mixture was chosen to mimic the typical phospholipid composition of the plasma membrane of *A. thaliana* (Berczi and Horvath 2003; Uemura et al. 1995). Static ^{31}P NMR spectra of the membrane lipids in the presence and in the absence of TWD1(335–365) exhibited very similar axially symmetric powder pattern line shapes revealing that the samples were in a lamellar liquid-crystalline phase state (Fig. 2a, b). The spectra could be simulated using a superposition of two axially symmetric powder spectra at an intensity ratio of 1:2, where the larger ^{31}P CSA was attributed to POPC-d_{31} and the smaller to POPE and POPG (Huster et al. 2002). Upon addition of TWD1(335–365) the ^{31}P CSA span values increased from 41.5 to 43.0 ppm for POPC-d_{31} and from 35.5 to 36.4 ppm for POPE/POPG, respectively. This result indicates only a minor influence of TWD1(335–365) on the lipid head groups given the experimental uncertainty of ±1 ppm.

Next we investigated the influence of TWD1(335–365) on lipid chain order and packing in mixed POPC-d_{31}/POPE/POPG membranes by ^{2}H NMR spectroscopy. Lipid order was reported from the perdeuterated *sn*-1 chain of POPC-d_{31}. The ^{2}H NMR spectra showed the typical superposition of Pake doublets of acyl chain methylene and methyl groups (Fig. 2c, d). Addition of TWD1(335–365) reduced the individual quadrupolar splittings by ∼2 to 5 kHz depending on the carbon position.

The peptide-induced differences in lipid order are best seen in plots of the order parameters versus chain segment position shown in Fig. 3. In the presence of TWD1(335–365) the chain order parameters are significantly decreased. The average order parameter of POPC-d_{31} in the mixed membrane drops from 0.179 to 0.154 after addition of TWD1(335–365). The decrease in order is more pronounced in the lower half of the palmitoyl chain of POPC. This can be best appreciated from the normalized order parameter difference, $\Delta S(n)/S(n)_{ref}$, of the order parameter profiles obtained with and without peptide present, which is shown in the inset of Fig. 3 (Henzler-Wildman et al. 2004). The most pronounced decrease in chain order occurs

around carbon position 11. The smaller effect of peptide incorporation on the order parameters of carbon segments beyond position 11 results simply from the permanently low order at the methyl end of the chain.

Conformation of TWD1(335–365) in a membrane environment

Typical ^{13}C MAS NMR spectra of specifically ^{13}C-labelled TWD1(335–365) in a phospholipid membrane environment are shown in Fig. 4. Narrow peaks refer to natural abundance ^{13}C signals of the lipids, while broader signals correspond to peptide resonances. At a temperature of 30°C most of the peptide signals are poorly resolved in the ^{13}C CP MAS spectrum (Fig. 4a) as well as in the directly polarized dipolar-decoupled ^{13}C MAS spectrum (Fig. 4b). Only one peak at 49.9 ppm shows significant intensity in the directly polarized ^{13}C spectrum, but is hardly observable in the CP spectrum. Based on isotropic chemical shift, this peak could be the Cα signal of Ala 364. The different appearance of the peak in directly and cross-polarized ^{13}C NMR spectra suggests that the site undergoes large amplitude motions on a fast time scale. Other peptide signals are largely absent in both types of spectra. Such difficulties in the detection of membrane-associated peptides have been reported previously and were attributed to microsecond time scale motions (Saitô et al. 2000; Smith et al. 1987; Warschawski et al. 1998).

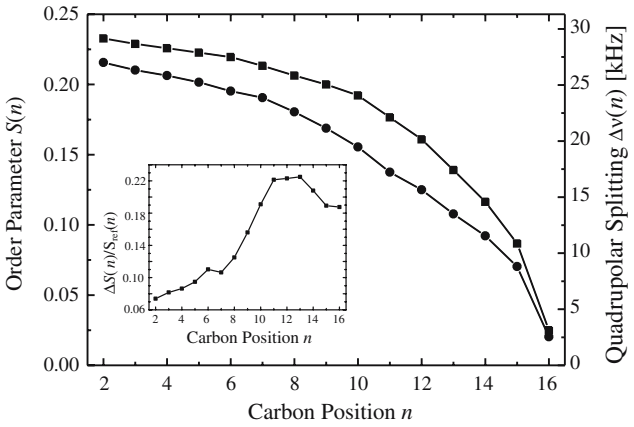

Fig. 3 Influence of the TWD1(335–365) peptide on lipid hydrocarbon chain order at 30°C. Smoothed ^{2}H NMR chain order parameter profiles and normalized difference order parameter profile $\Delta S(n)/S_{ref}(n)$ (*inset*) of POPC-d_{31}/POPE/POPG (molar ratio 1:1:1) membranes obtained in the absence (*filled square*) and in the presence (*filled circle*) of 3.2 mol% TWD1(335–365) are presented. The *vertical scale* on the *right* shows the measured quadrupolar splittings, $\Delta\nu_Q(n)$. The normalized order parameter difference indicates the fractional change in order parameter at each position along the acyl chain upon addition of TWD1(335–365). The values are positive, indicating that the presence of TWD1(335–365) induces a decrease in the chain order of the membrane

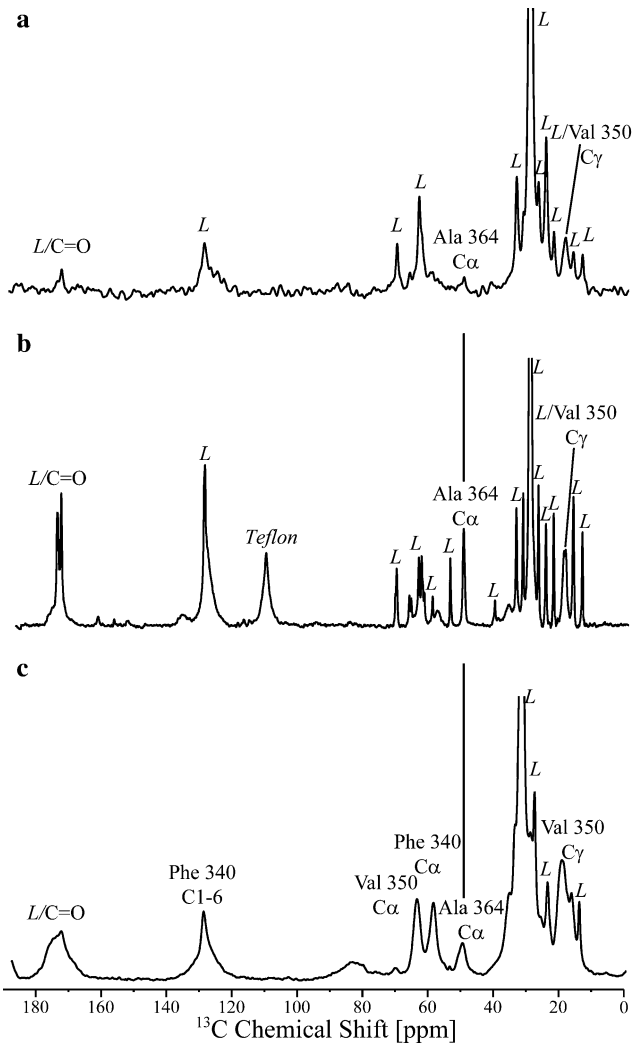

Fig. 4 188.5 MHz ^{13}C MAS NMR spectra of 3.2 mol% TWD1(335–365) in POPC-d_{31}/POPE/POPG membranes (1:1:1, mol/mol/mol) containing 35 wt% buffer. The CP MAS spectrum (**a**) and the directly polarized MAS spectrum (**b**) were recorded at 30°C and 7,000 Hz MAS frequency. The CP MAS spectrum below (**c**) was obtained at −30°C and 8,333 Hz. Assigned peptide resonances are annotated. Lipid signals are denoted by "*L*"

These problems can be overcome by freezing the sample to −30°C. At this temperature all peptide motions except for the fast methyl group rotations are frozen out, leading to the ^{13}C CP MAS spectrum shown in Fig. 4c. Now the peptide peaks dominate the NMR spectrum due to the isotopic enrichment. In particular the three Cα signals of the peptide are clearly visible. It is interesting to note that the chemical shift values of those peptide signals that could be observed at 30°C did not shift upon freezing indicating that the peptide conformation has not changed either.

Resonance assignment is a prerequisite for any structural investigation by NMR. 2D ^{13}C–^{13}C correlation spectra were acquired to detect the connectivities within the spin system of the labelled amino acids. A contour plot of a proton-driven ^{13}C spin diffusion spectrum at −30°C with a mixing time of 100 ms is shown in Fig. 5a. Correlations between ^{13}C spins over up to three bonds are visible. This allows identification of all ^{13}C peptide signals of the three labelled amino acids of TWD1(335–365), while all natural abundance signals do not show correlation peaks. Alternatively, correlation spectra devoid of diagonal peaks can be acquired using single quantum/double quantum correlation techniques of the INADEQUATE type (Fig. 5b), providing simple and easy to analyse NMR spectra.

Isotropic chemical shifts are sensitive markers of protein secondary structure (Igumenova et al. 2004; Luca et al. 2001; Saitô 1986; Spera and Bax 1991; Wishart and Sykes 1994). Cα and CO ^{13}C resonances exhibit a downfield shift relative to random coil values in α-helices and an upfield shift in β-sheets. Cβ chemical shifts move in the opposite direction upon secondary structure formation. The isotropic chemical shifts of the three labelled amino acids of TWD1(335–365) obtained from ^{13}C MAS NMR are shown in Table 1. Referencing of chemical shifts is still challenging in solid-state NMR due to the lack of internal standards (Morcombe and Zilm 2003). Therefore, we also report the Cα–Cβ chemical shift differences, which are independent of referencing (Luca et al. 2001). Comparison of the isotropic chemical shift of Phe 340 and Val 350 with secondary structure specific ranges strongly suggests an α-helical structure of these two residues and supports an α-helical conformation of the central part of TWD1(335–365), while Ala 364 at the C-terminal end of the TWD1-peptide is random coil based on the isotropic chemical shifts and has a relatively high mobility.

Membrane topology of TWD1(335–365)

Static ^{15}N NMR spectra of TWD1(335–365) peptide in macroscopically oriented membranes with the same phospholipids composition as above were recorded to study helix orientation relative to the membrane. The degree of orientation of the phospholipid bilayers aligned between stacked glass plates was checked by ^{31}P NMR at orientations of 0° and 90° between the membrane normal and the magnetic field (data not shown). A high degree of membrane orientation was confirmed. During the ^{15}N NMR measurements the lipid bilayers were oriented with their normal parallel to the external magnetic flied.

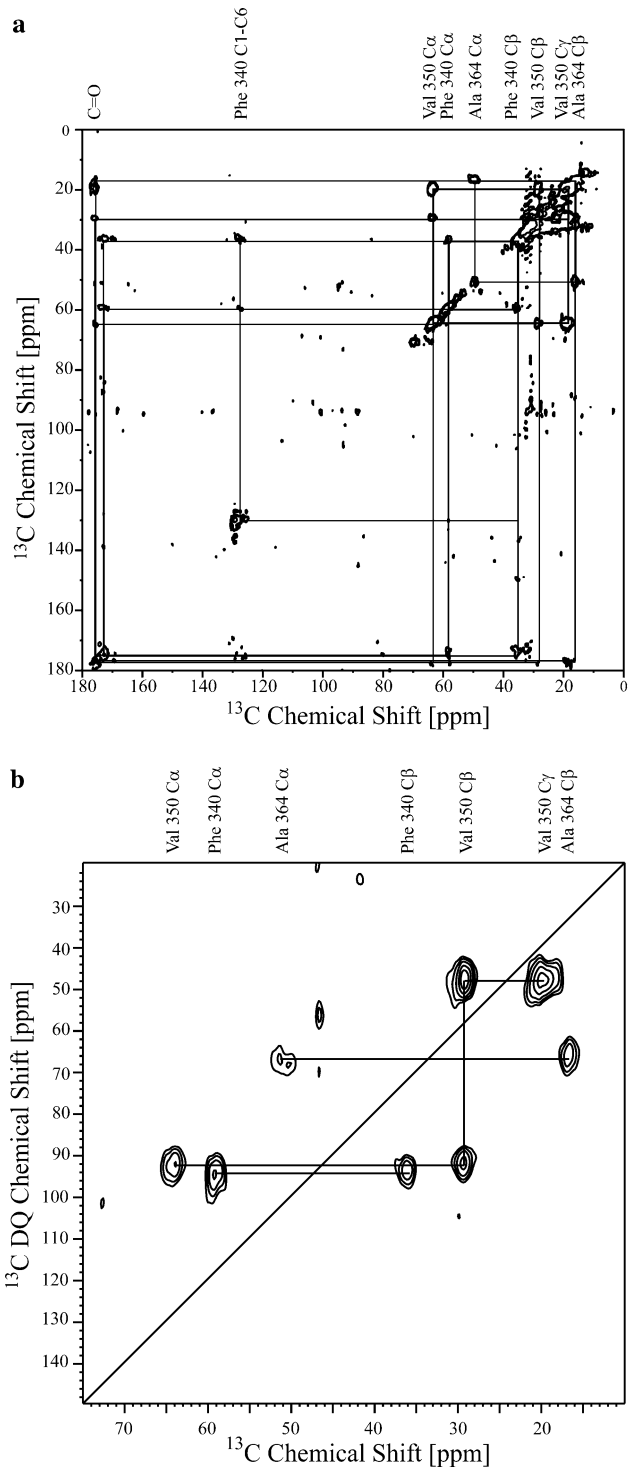

Fig. 5 Contour plots of a ^{13}C–^{13}C correlation spectrum employing proton-driven ^{13}C spin diffusion at a mixing time of 100 ms (**a**) and of a ^{13}C single quantum/double quantum correlation spectrum of the INADEQUATE type (**b**) of 3.2 mol% TWD1(335–365) in POPC-d_{31}/POPE/POPG membranes (1:1:1, mol/mol/mol) containing 35 wt% buffer. Spectra were acquired at a MAS frequency of 8,333 Hz at −30°C. Correlations between the assigned signals of the isotopically labelled amino acids are *highlighted*

Table 1 Isotropic ^{13}C chemical shift values (in ppm relative to TMS) of TWD1(335–365) residues in a membrane environment determined from ^{13}C–^{13}C correlation spectra

	$^{13}C\alpha$	$^{13}C\beta$	$^{13}C\alpha$–$^{13}C\beta$	^{13}CO
Phe 340[a]	58.5 ± 0.3	36.1 ± 0.3	22.4 ± 0.6	173.5 ± 0.3
Val 350[b]	63.9 ± 0.2	28.5 ± 0.4	35.4 ± 0.6	175.5 ± 0.3
Ala 364[c]	49.9 ± 0.2	16.4 ± 0.2	33.5 ± 0.4	175.5 ± 0.3

[a] Average ^{13}C chemical shifts for Phe in α-helix structures are 58.6, 36.7, and 174.9 ppm for Cα, Cβ, and CO, respectively

[b] Average ^{13}C chemical shifts for Val in α-helix structures are 63.0, 29.9, and 175.8 ppm for Cα, Cβ, and CO, respectively

[c] Average ^{13}C chemical shifts for Ala in coil structures are 50.1, 17.3, and 174.8 ppm for Cα, Cβ, and CO, respectively

The ^{15}N NMR spectrum of TWD1(335–365) in oriented lipid membranes is shown in Fig. 6c. For comparison, the ^{15}N NMR spectra of crystalline TWD1(335–365) and ^{15}N-labelled TWD1(335–365) in multilamellar POPC/POPE/POPG vesicles are presented in Fig. 6a, b, respectively. The ^{15}N NMR spectrum of crystalline TWD1(335–365) was simulated using an ^{15}N chemical shift anisotropy of $\Delta\sigma = 163.5$ ppm and an asymmetry parameter of $\eta = 0.21$.

The ^{15}N NMR spectrum of TWD1(335–365) in oriented membranes exhibits a relatively broad peak at ~80 ppm. The backbone N–H bond vectors in an α-helix are approximately parallel to both the helix axis and the main axis of the almost axially symmetric ^{15}N chemical shift tensor. Such an ^{15}N spectrum of TWD1(335–365) in oriented membranes is indicative of an orientation of the α-helix perpendicular to the magnetic field and to the membrane normal (Hashimoto et al. 1999; Lee et al. 1999; Marassi et al. 1999). The small downfield shoulder in Fig. 6c can be most likely assigned to Ala 364, which is not part of the α-helix based on ^{13}C chemical shift data. Because of the higher flexibility and mobility of this part of the peptide the ^{15}N chemical shift of this residue is shifted to more isotropic values.

The line width of ~32 ppm (without the downfield shoulder) in the ^{15}N NMR spectrum of oriented TWD1(335–365) is a bit larger compared to the literature values of well-oriented membrane proteins, which typically exhibit line widths of ~10 to 20 ppm (Bechinger et al. 2004; Ramamoorthy et al. 2004). One contribution to the increased line width could be a slightly different membrane orientation of Val 350 and Phe 340 in the α-helix. While the former should be located in the centre of the α-helix, Phe 340 is situated at the beginning of the helix and might therefore not exhibit perfect helical geometry. The second contribution are very likely motions on the microsecond time scale that had already been suspected from the ^{13}C MAS NMR spectra at 30°C. This supposition was confirmed by the NMR spectrum of TWD1(335–365) in multilamellar lipid vesicles (Fig. 6b). The low signal-to-noise ratio and complicated spectral line shape are typical features of the presence of intermediate timescale peptide motions (Wasniewski et al. 2004). Nevertheless, comparison of the oriented and powder ^{15}N NMR spectra of TWD1(335–365) in membrane environment clearly rules out that the oriented spectrum has contributions from unaligned peptides.

Discussion

The current manuscript addresses the membrane structure and topology of the C-terminal fragment (residues 335–365) of the protein TWD1 from *A. thaliana*. Advanced software tools allow prediction of TM helices from protein amino acid sequence with high fidelity based on combinations of diverse TM helix signals including hydrophobicity, charge bias, helix length, and the correct order of typical membrane protein domains (Krogh et al. 2001). Analysis of the TWD1 sequence indicates a strong tendency of the amino acid stretch from residue 338 or 339 to residue 357 to form a TM helix and it was speculated that the C-terminus of TWD1 might serve as membrane anchor (Kamphausen et al. 2002).

Our solid-state NMR results confirm membrane association of peptide TWD1(335–365) and suggest formation of an α-helix in the central hydrophobic region of the peptide. However, in contrast to first intuition the long axis of the helix is oriented parallel to the lipid water interface rather than being transmembrane. In what follows we discuss the peptide amino acid sequence for signs regarding its membrane topology.

White and Wimley established two experiment-based hydrophobicity scales, which allow estimation of the free energy cost/gain of transferring a peptide from buffer to a membrane or a membrane interface (White and Wimley 1998; Wimley and White 1996). The whole-residue free energy of transfer of non-hydrogen-bonded amino acid residues from water to the interface of a POPC membrane is specified by the interface-scale. The other scale is based on amino acid side chain

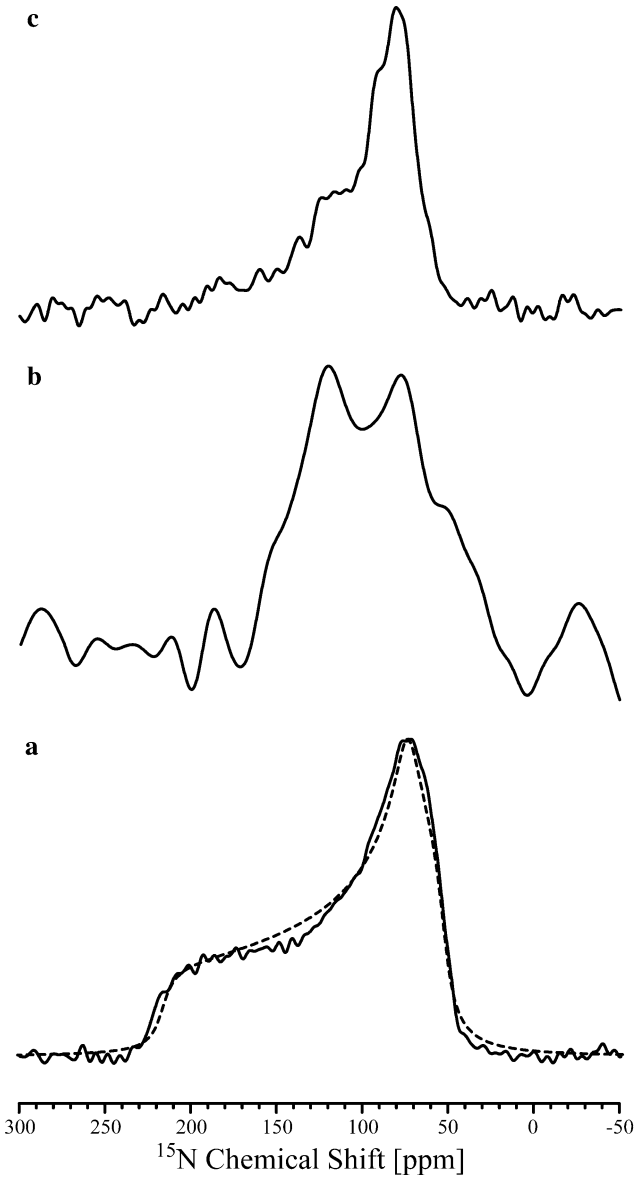

Fig. 6 Static ^{15}N NMR spectra (*solid lines*) of non-oriented crystalline TWD1(335–365) (**a**), 3.2 mol% TWD1(335–365) in multilamellar POPC/POPE/POPG vesicles (1:1:1, mol/mol/mol) hydrated with 35 wt% buffer (**b**), and of 3.2 mol% TWD1(335–365) in oriented POPC/POPE/POPG bilayers (1:1:1, mol/mol/mol) hydrated at 98% relative humidity and oriented with the membrane normal parallel to the field of the NMR magnet (**c**). Spectra were measured at 30°C. The powder spectrum of crystalline TWD1(335–365) was simulated using the parameters σ_{11} = 53.3 ppm, σ_{22} = 74.4 ppm and σ_{33} = 216.8 ppm (*dashed line* in **a**)

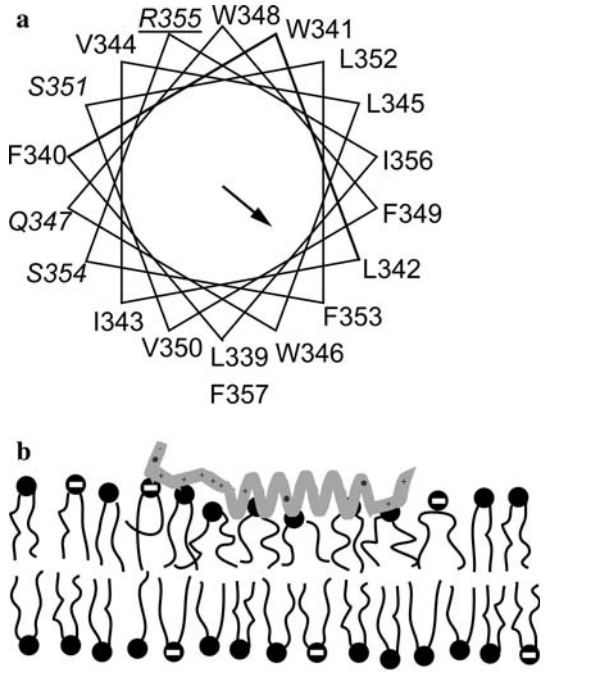

Fig. 7 Summary of the structural data obtained in this work. **a** Helical wheel representation of the central hydrophobic residues 339–357. Charged residues are *underlined* and the polar amino acids are *italicised*. The direction of the hydrophobic moment of the α-helix is given by an *arrow*. **b** The cartoon summarizes our structural model of TWD1(335–365) in a lipid membrane. The positions of the isotopically labelled and charged amino acids are *highlighted*

contributions determined from water–octanol partition coefficients and a uniform backbone contribution that accounts for the transfer of a hydrogen-bonded peptide bond from water to a non-polar environment. These experimental hydrophobicity scales have proven extremely useful for the understanding of peptide partitioning into membranes. For instance, the octanol-scale was successfully used for close to 100% correct identification of TM helices in a large sample of membrane proteins with known crystal structures (Jayasinghe et al. 2001).

The favourable free energy of transferring the hydrophobic fragment of TWD1 comprising residues 339–357 yields $\Delta G = -74.5$ and -46.4 kJ/mol for the octanol- and interface-scale, respectively. These ΔG values are among the most negative on the Wimley White scale that have been reported for known TM and interfacial helices (Jayasinghe et al. 2001; White and Wimley 1999). Apparently the hydrophobic effect is a major driving force for partitioning this peptide into the membrane. Folding would further increase the free energy gain of peptide transfer into the interface by approximately -1.7 kJ/mol per H-bonded residue (Ladokhin and White 1999). Hydrophobicity analysis alone cannot unambiguously distinguish between TM and interfacial peptide deposition in the membrane. For example, electrostatic interactions of the peptide with charged lipids are not considered, the influence of peptide insertion on the free energy of the lipid bilayer is reflected to some extend in the interface but not

explicitly in the octanol-scale. Environmental conditions like pH, ionic strength, or temperature may modify the actual ΔG as well. Nevertheless, the hydrophobicity scale based analysis indicates that embedding the peptide fragment 339–357 in the membrane is thermodynamically extremely favourable.

Statistical analysis of TM helices reveals preferred positions of some amino acids along the membrane normal (Ulmschneider et al. 2005; Wallin et al. 1997; White and Wimley 1999). The central part of a TM helix contains predominantly aliphatic and phenylalanine residues while amidated and charged residues are restraint to helix-flanking and solvent exposed regions. The polar aromatic residues show a clear preference for the membrane interface (Schiffer et al. 1992; Yau et al. 1998). The fragment TWD1(339–357) would perfectly span the hydrophobic core of the membrane with the exception that three polar residues (Trp 346, Gln 347, Trp 348) would reside in the centre of the TM helix.

The tendency of an α-helix to assume a preferred orientation at the interface between a polar and an apolar medium is related to helix amphipathicity (Eisenberg et al. 1982). The helical wheel representation of the helical fragment TWD1(339–357) is shown in Fig. 7a. The charged Arg 355 and most of the polar residues (Gln 347, Ser 351/354, Trp 341/348) are located on one side of the wheel while aliphatic residues dominate the opposite side. A more quantitative analysis can be based on the sequence hydrophobic moment, μ_H, which is the sum of the projections of the hydrophobicity vectors of the amino acid residues in a plane perpendicular to the helix axis (Eisenberg et al. 1984). The 19 residue fragment TWD1(339–357) has considerable amphipathicity ($\langle\mu_H\rangle = 1.57$ kJ/mol). In the hydrophobic moment plot (Eisenberg et al. 1989) it is situated at the boundary separating the clusters of TM and surface exposed helices.

Clearly, only experimental data can provide unambiguous information about the structure and topology of the membrane anchor of TWD1. Here we have used static and MAS solid-state NMR techniques to determine a structural model of membrane bound TWD1(335–365).

The ^{13}C isotropic chemical shift data strongly suggest an α-helical conformation of Phe 340 and Val 350 in the central part of TWD1(335–365). Formation of a hydrogen-bonded α-helix reduces the polarity of this peptide domain and enhances the probability for peptide interaction with the phospholipid membrane (White and Wimley 1998). The multiple charged C-terminus is most likely unstructured. The ^{13}C chemical shift of Ala 364 is indicative of a random coil. Formation of secondary structure in this region is most likely inhibited by electrostatic interactions of the four positively charged amino acids.

Binding of the peptide to the membrane causes only moderate changes of membrane structure. The static ^{31}P NMR measurements reveal no alterations of lipid headgroup structure due to association of TWD1(335–365) with the membrane.

The ^{2}H NMR results are compatible with both a transmembrane and a surface orientation of the TWD1(335–365) α-helix. In the first case, the thickness of the hydrophobic bilayer core may need adjustment (by increasing or decreasing the lipid chain order) to the length of the membrane spanning hydrophobic segment of the TM α-helix to account for hydrophobic mismatch (Killian 1998; Mouritsen and Bloom 1984). The observed decrease of lipid chain ^{2}H NMR order parameters in the presence of TWD1(335–365) would indicate membrane thinning. In the second case, the decrease of order parameters (particularly in the lower chain region) would be due to embedding the amphipathic α-helix in the lipid water interface region of the membrane. Molecular crowding at the interface modifies the lateral lipid organization. Additional space opens up further down the chains, which is occupied by larger amplitudes of motion in the membrane centre resulting in lower order parameters (Barré et al. 2003; Koenig et al. 1999). A similar model was recently suggested for the amphipathic α-helical peptides LL-37 and MSI-78, which are also located in the membrane interface (Henzler-Wildman et al. 2004; Mecke et al. 2005). In these studies also a decrease in the ^{2}H NMR lipid order parameter was observed upon peptide binding. In addition, a membrane thinning effect was found by AFM measurements for MSI-78 in agreement with the lower order parameters induced by peptide binding to the membrane interface (Mecke et al. 2005).

The static ^{15}N NMR measurements clearly indicate that TWD1(335–365) adopts an orientation perpendicular to the bilayer normal. The reduced ^{2}H NMR chain order parameters are due to incorporation of the amphipathic peptide in the lipid water interface region with the helix axis aligned parallel to the membrane surface and aliphatic side chains penetrating deeper into the membrane. The Trp fluorescence signal of TWD1(335–365) in membranes exhibits a blue shift also indicating that these residues reside in an apolar environment (unpublished results).

The large line width of the ^{15}N NMR spectra and the inefficient polarization transfer via CP at 30°C, particularly for Phe 340 and Val 350, which are part of the α-helix, suggest motions of this peptide segment in the microsecond time window. This was confirmed

by the low signal to noise ratio and the specific line shape of the ^{15}N NMR spectra of TWD1(335–365) in multilamellar lipid vesicles. Interference between the molecular dynamics of the peptide and the applied coherent manipulations of nuclear magnetization (both by radiofrequency pulses and mechanical sample rotation) contributes to line broadening and prevents detection of ^{13}C NMR signals. Such motions are particularly frequent for transmembrane α-helices (Warschawski et al. 1998) but have also been observed for segments of larger membrane proteins such as bacteriorhodopsin (Saitô et al. 2000) and rhodopsin (Smith et al. 1987). However, we are not yet in a position to suggest a particular mode of microsecond time scale motion of membrane bound TWD1(335–365) based on the limited set of data determined in this study. Cooling the sample to −30°C abolishes the intermediate time scale motions and leads to efficient CP magnetization transfer and fully resolved NMR signals of the three ^{13}C-labelled amino acids of TWD1(335–365). Ala 364 at the unstructured C-terminal end of TWD1(335–365) is subject to a different dynamic regime involving faster motions with large amplitude. The high molecular dynamics of the peptide in the membrane also strongly argues against peptide oligomerization.

Our data suggest that TWD1(335–365) adopts an amphipathic α-helical structure, which is located in the lipid water interface of the membrane. The cartoon shown in Fig. 7b summarizes the structural model for membrane bound TWD1(335–365). The hydrophobic effect is the major driving force for helix association with the membrane. Formation of a hydrogen-bonded α-helix in the central hydrophobic region of the peptide (amino acids 339–357) lowers the free energy cost of placing polar peptide bonds in an environment of reduced polarity. Electrostatic interactions between the positively charged amino acids at both ends of the TWD1(335–365) sequence and the negatively charged headgroups of the phospholipid molecules provide additional contributions to the binding energy.

To the best of our knowledge, a lipid water interface-associated amphipathic helix alone is insufficient for permanent membrane anchoring of a protein. Very likely, additional factors must strengthen association of full-length TWD1 with the membrane. In the recent literature, a C-terminal GPI anchor has been discussed for TWD1 (Geisler and Murphy 2006), which could provide the permanent membrane anchor for the protein. However, so far there is no experimental proof for such a modification of TWD1.

But there are also alternative ways to explain the preference of TWD1 for the membrane. There are strong indications that TWD1 functions as part of multi-protein complexes where it plays a regulatory role in polar auxin transport (Geisler et al. 2003; Geisler and Murphy 2006). Specific interactions of TWD1 with membrane spanning ABC transporters or with other components of the complex could very well account for the reported association of TWD1 with membranes. Experimentally tractable models reduce the complexity of a biological system. By their very nature they lack some components of the molecular machinery of a living cell, which may have an impact on the processes studied. Understanding of translocon-mediated insertion of polypeptide chains emerging from the ribosome has dramatically improved over the past few years (White and von Heijne 2005). Interestingly, the biological code used by the translocon to select amino acid stretches for deposition into the membrane is closely related to the thermodynamic hydrophobicity scales of Wimley and White (Hessa et al. 2005). The very large mean hydrophobicity of residues 339–357 of TWD1 makes this stretch a good candidate for translocon-guided membrane insertion. Clearly, biochemical experiments would be necessary to evaluate this hypothesis.

Acknowledgments The study was supported by the Deutsche Forschungsgemeinschaft (HU 720/5-1 and 5-2) and (KO 2143/3-2).

References

Afonin S, Durr UH, Glaser RW, Ulrich AS (2004) 'Boomerang'-like insertion of a fusogenic peptide in a lipid membrane revealed by solid-state ^{19}F NMR. Magn Reson Chem 42:195–203

Andronesi OC, Becker S, Seidel K, Heise H, Young HS, Baldus M (2005) Determination of membrane protein structure and dynamics by magic-angle-spinning solid-state NMR spectroscopy. J Am Chem Soc 127:12965–12974

Barré P, Zschörnig O, Arnold K, Huster D (2003) Structural and dynamical changes of the bindin B18 peptide upon binding to lipid membranes. A solid-state NMR study. Biochemistry 42:8377–8386

Bechinger B (1999) The structure, dynamics and orientation of antimicrobial peptides in membranes by multidimensional solid-state NMR spectroscopy. Biochim Biophys Acta 1462:157–183

Bechinger B, Aisenbrey C, Bertani P (2004) The alignment, structure and dynamics of membrane-associated polypeptides by solid-state NMR spectroscopy. Biochim Biophys Acta 1666:190–204

Bennett AE, Rienstra CM, Auger M, Lakshmi KV, Griffin RG (1995) Heteronuclear decoupling in rotating solids. J Chem Phys 103:6951–6958

Berczi A, Horvath G (2003) Lipid rafts in the plant plasma membrane? Acta Biol Szeged 47:7–10

Casey PJ (1995) Protein lipidation in cell signaling. Science 268:221–225

Davis JH, Auger M (1999) Static and magic angle spinning NMR of membrane peptides and proteins. Prog Nucl Magn Reson Spectrosc 35:1–84

Davis JH, Jeffrey KR, Bloom M, Valic MI, Higgs TP (1976) Quadrupolar echo deuteron magnetic resonance spectroscopy in ordered hydrocarbon chains. Chem Phys Lett 42:390–394

Eckhoff A, Granzin J, Kamphausen T, Büldt G, Schulz B, Weiergraber OH (2005) Crystallization and preliminary X-ray analysis of immunophilin-like FKBP42 from *Arabidopsis thaliana*. Acta Crystallograph Sect F Struct Biol Cryst Commun 61:363–365

Eisenberg D, Weiss RM, Terwilliger TC (1982) The helical hydrophobic moment: a measure of the amphiphilicity of a helix. Nature 299:371–374

Eisenberg D, Weiss RM, Terwilliger TC (1984) The hydrophobic moment detects periodicity in protein hydrophobicity. Proc Natl Acad Sci USA 81:140–144

Eisenberg D, Wesson M, Wilcox W (1989) Hydrophobic moments as tools for analyzing protein sequences and structures. In: Fasman GD (ed) Prediction of protein structure and the principles of protein conformation. Plenum Press, New York, London, pp 635–646

Geisler M, Murphy AS (2006) The ABC of auxin transport: the role of *p*-glycoproteins in plant development. FEBS Lett 580:1094–1102

Geisler M, Kolukisaoglu HU, Bouchard R, Billion K, Berger J, Saal B, Frangne N, Koncz-Kalman Z, Koncz C, Dudler R, Blakeslee JJ, Murphy AS, Martinoia E, Schulz B (2003) TWISTED DWARF1, a unique plasma membrane-anchored immunophilin-like protein, interacts with *Arabidopsis* multidrug resistance-like transporters AtPGP1 and AtPGP19. Mol Biol Cell 14:4238–4249

Geisler M, Girin M, Brandt S, Vincenzetti V, Plaza S, Paris N, Kobae Y, Maeshima M, Billion K, Kolukisaoglu UH, Schulz B, Martinoia E (2004) *Arabidopsis* immunophilin-like TWD1 functionally interacts with vacuolar ABC transporters. Mol Biol Cell 15:3393–3405

Hahn EL (1950) Spin echoes. Phys Rev 80:580–594

Hancock JF, Cadwallader K, Paterson H, Marshall CJ (1991) A CAAX or a CAAL motif and a second signal are sufficient for plasma membrane targeting of ras proteins. EMBO J 10:4033–4039

Hashimoto Y, Toma K, Nishikido J, Yamamoto K, Haneda K, Inazu T, Valentine KG, Opella SJ (1999) Effects of glycosylation on the structure and dynamics of eel calcitonin in micelles and lipid bilayers determined by nuclear magnetic resonance spectroscopy. Biochemistry 38:8377–8384

Henzler-Wildman KA, Lee DK, Ramamoorthy A (2003) Mechanism of lipid bilayer disruption by the human antimicrobial peptide, LL-37. Biochemistry 42:6545–6558

Henzler-Wildman KA, Martinez GV, Brown MF, Ramamoorthy A (2004) Perturbation of the hydrophobic core of lipid bilayers by the human antimicrobial peptide LL-37. Biochemistry 43:8459–8469

Hessa T, Kim H, Bihlmaier K, Lundin C, Boekel J, Andersson H, Nilsson I, White SH, von Heijne G (2005) Recognition of transmembrane helices by the endoplasmic reticulum translocon. Nature 433:377–381

Hohwy M, Rienstra CM, Jaroniec CP, Griffin RG (1999) Fivefold symmetric homonuclear dipolar recoupling in rotating solids: application to double quantum spectroscopy. J Chem Phys 110:7983–7992

Huster D (2005) Investigations of the structure and dynamics of membrane-associated peptides by magic angle spinning NMR. Prog Nucl Magn Reson Spectrosc 46:79–107

Huster D, Arnold K, Gawrisch K (1998) Influence of docosahexaenoic acid and cholesterol on lateral lipid organization in phospholipid mixtures. Biochemistry 37:17299–17308

Huster D, Yao X, Jakes KS, Hong M (2002) Conformational changes of colicin Ia channel-forming domain upon membrane binding: a solid-state NMR study. Biochim Biophys Acta 1561:159–170

Huster D, Vogel A, Katzka C, Scheidt HA, Binder H, Dante S, Gutberlet T, Zschörnig O, Waldmann H, Arnold K (2003) Membrane insertion of a lipidated ras peptide studied by FT-IR, solid-state NMR, and neutron diffraction spectroscopy. J Am Chem Soc 125:4070–4079

Igumenova TI, Wand AJ, McDermott AE (2004) Assignment of the backbone resonances for microcrystalline ubiquitin. J Am Chem Soc 126:5323–5331

Ikezawa H (2002) Glycosylphosphatidylinositol (GPI)-anchored proteins. Biol Pharm Bull 25:409–417

Jayasinghe S, Hristova K, White SH (2001) Energetics, stability, and prediction of transmembrane helices. J Mol Biol 312:927–934

Kamphausen T, Fanghanel J, Neumann D, Schulz B, Rahfeld JU (2002) Characterization of *Arabidopsis thaliana* AtFKBP42 that is membrane-bound and interacts with Hsp90. Plant J 32:263–276

Ketchem RR, Hu W, Cross TA (1993) High-resolution conformation of gramicidin A in a lipid bilayer by solid-state NMR. Science 261:1457–1460

Killian JA (1998) Hydrophobic mismatch between proteins and lipids in membranes. Biochim Biophys Acta 1376:401–415

Koenig BW, Ferretti JA, Gawrisch K (1999) Site-specific deuterium order parameters and membrane-bound behavior of a peptide fragment from the intracellular domain of HIV-1 gp41. Biochemistry 38:6327–6334

Krogh A, Larsson B, von Heijne G, Sonnhammer EL (2001) Predicting transmembrane protein topology with a hidden Markov model: application to complete genomes. J Mol Biol 305:567–580

Ladokhin AS, White SH (1999) Folding of amphipathic alpha-helices on membranes: energetics of helix formation by melittin. J Mol Biol 285:1363–1369

Lafleur M, Fine B, Sternin E, Cullis PR, Bloom M (1989) Smoothed orientational order profile of lipid bilayers by ^{2}H-nuclear magnetic resonance. Biophys J 56:1037–1041

Lee DK, Santos JS, Ramamoorthy A (1999) Application of one-dimensional dipolar shift solid-state NMR spectroscopy to study the backbone conformation of membrane-associated peptides in phospholipid bilayers. J Phys Chem B 103:8383–8390

Luca S, Filippov DV, van Boom JH, Oschkinat H, de Groot HJ, Baldus M (2001) Secondary chemical shifts in immobilized peptides and proteins: a qualitative basis for structure refinement under magic angle spinning. J Biomol NMR 20:325–331

Luca S, Heise H, Baldus M (2003) High-resolution solid-state NMR applied to polypeptides and membrane proteins. Acc Chem Res 36:858–865

Marassi FM, Ma C, Gratkowski H, Straus SK, Strebel K, Oblatt-Montal M, Montal M, Opella SJ (1999) Correlation of the structural and functional domains in the membrane protein Vpu from HIV-1. Proc Natl Acad Sci USA 96:14336–14341

Marshall CJ (1993) Protein prenylation: a mediator of protein–protein interactions. Science 259:1865–1866

Mecke A, Lee DK, Ramamoorthy A, Orr BG, Banaszak Holl MM (2005) Membrane thinning due to antimicrobial peptide binding: an atomic force microscopy study of MSI-78 in lipid bilayers. Biophys J 89:4043–4050

Morcombe CR, Zilm KW (2003) Chemical shift referencing in MAS solid state NMR. J Magn Reson 162:479–486

Mouritsen OG, Bloom M (1984) Mattress model of lipid–protein interactions in membranes. Biophys J 46:141–153

Murray D, Ben-Tal N, Honig B, McLaughlin S (1997) Electrostatic interaction of myristoylated proteins with membranes: simple physics, complicated biology. Structure 5:985–989

Opella SJ, Marassi FM (2004) Structure determination of membrane proteins by NMR spectroscopy. Chem Rev 104:3587–3606

Porcelli F, Buck-Koehntop BA, Thennarasu S, Ramamoorthy A, Veglia G (2006) Structures of the dimeric and monomeric variants of magainin antimicrobial peptides (MSI-78 and MSI-594) in micelles and bilayers, determined by NMR spectroscopy. Biochemistry 45:5793–5799

Ramamoorthy A, Wei YF, Lee DK (2004) PISEMA solid-state NMR spectroscopy. Ann Rep NMR Spectrosc 52:1–52

Reuther G, Tan K-T, Köhler J, Nowak C, Pampel A, Arnold K, Kuhlmann J, Waldmann H, Huster D (2006) Structural model of the membrane-bound C terminus of lipid-modified human N-ras protein. Angew Chem Int Ed Engl 45:5387–5390

Saitô H (1986) Conformation-dependent ^{13}C chemical shifts: a new means of conformational characterization as obtained by high-resolution solid-state ^{13}C NMR. Magn Reson Chem 24:835–852

Saitô H, Tuzi S, Yamaguchi S, Tanio M, Naito A (2000) Conformation and backbone dynamics of bacteriorhodopsin revealed by ^{13}C-NMR. Biochim Biophys Acta 1460:39–48

Schiffer M, Chang CH, Stevens FJ (1992) The functions of tryptophan residues in membrane proteins. Protein Eng 5:213–214

Seul M, Sammon MJ (1990) Preparation of urfactant multilayer films on solid substrates by deposition from organic solution. Thin Solid Films 185:287–305

Sharpe S, Yau WM, Tycko R (2006) Structure and dynamics of the HIV-1 Vpu transmembrane domain revealed by solid-state NMR with magic-angle spinning. Biochemistry 45:918–933

Smith SO, Palings I, Copie V, Raleigh DP, Courtin J, Pardoen JA, Lugtenburg J, Mathies RA, Griffin RG (1987) Low-temperature solid-state ^{13}C NMR studies of the retinal chromophore in rhodopsin. Biochemistry 26:1606–1611

Smith SO, Song D, Shekar S, Groesbeek M, Ziliox M, Aimoto S (2001) Structure of the transmembrane dimer interface of glycophorin A in membrane bilayers. Biochemistry 40:6553–6558

Spera S, Bax A (1991) Empirical correlation between protein backbone conformation and Cα and Cβ ^{13}C nuclear magnetic resonance chemical shifts. J Am Chem Soc 113:5490–5492

Szeverenyi NM, Sullivan MJ, Maciel GE (1982) Observation of spin exchange by two-dimensional Fourier transform ^{13}C cross polarization magic-angle spinning. J Magn Reson 47:462–475

Thompson LK (2002) Solid-state NMR studies of the structure and mechanisms of proteins. Curr Opin Struct Biol 12:661–669

Torres J, Stevens TJ, Samso M (2003) Membrane proteins: the 'Wild West' of structural biology. Trends Biochem Sci 28:137–144

Uemura M, Joseph RA, Steponkus PL (1995) Cold Acclimation of *Arabidopsis thaliana* (effect on plasma membrane lipid composition and freeze-induced lesions). Plant Physiol 109:15–30

Ulmschneider MB, Sansom MS, Di NA (2005) Properties of integral membrane protein structures: derivation of an implicit membrane potential. Proteins 59:252–265

Wagner K, Beck-Sickinger AG, Huster D (2004) Structural investigations of a human calcitonin-derived carrier peptide in membrane environment by solid-state NMR. Biochemistry 43:12459–81246

Wallin E, Tsukihara T, Yoshikawa S, von Heijne G, Elofsson A (1997) Architecture of helix bundle membrane proteins: an analysis of cytochrome *c* oxidase from bovine mitochondria. Protein Sci 6:808–815

Warschawski DE, Gross JD, Griffin RG (1998) Effects of membrane peptide dynamics on high-resolution magic-angle spinning NMR. J Chim Phys 95:460–466

Wasniewski CM, Parkanzky PD, Bodner ML, Weliky DP (2004) Solid-state nuclear magnetic resonance studies of HIV and influenza fusion peptide orientations in membrane bilayers using stacked glass plate samples. Chem Phys Lipids 132:89–100

Weiergraber OH, Eckhoff A, Granzin J (2006) Crystal structure of a plant immunophilin domain involved in regulation of MDR-type ABC transporters. FEBS Lett 580:251–255

White SH, von Heijne G (2005) Transmembrane helices before, during, and after insertion. Curr Opin Struct Biol 15:378–386

White SH, Wimley WC (1998) Hydrophobic interactions of peptides with membrane interfaces. Biochim Biophys Acta 1376:339–352

White SH, Wimley WC (1999) Membrane protein folding and stability: physical principles. Annu Rev Biophys Biomol Struct 28:319–365

Wimley WC, White SH (1996) Experimentally determined hydrophobicity scale for proteins at membrane interfaces. Nat Struct Biol 3:842–848

Wishart DS, Sykes BD (1994) Chemical shifts as a tool for structure determination. Methods Enzymol 239:363–392

Yang J, Weliky DP (2003) Solid-state nuclear magnetic resonance evidence for parallel and antiparallel strand arrangements in the membrane-associated HIV-1 fusion peptide. Biochemistry 42:11879–11890

Yau WM, Wimley WC, Gawrisch K, White SH (1998) The preference of tryptophan for membrane interfaces. Biochemistry 37:14713–14718

Zhang W, Crocker E, McLaughlin S, Smith SO (2003) Binding of peptides with basic and aromatic residues to bilayer membranes: phenylalanine in the MARCKS effector domain penetrates into the hydrophobic core of the bilayer. J Biol Chem 278:21459–21466